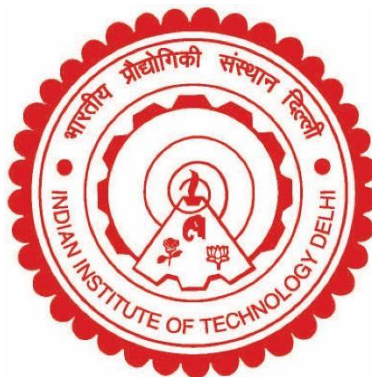


**DISPERSION OF VEHICULAR EXHAUST EMISSIONS IN
NEAR-FIELD REGION AROUND FLYOVER IN AN
ENVIRONMENTAL WIND TUNNEL**

S. JITENDRA PAL



**DEPARTMENT OF CIVIL ENGINEERING
INDIAN INSTITUTE OF TECHNOLOGY DELHI**

OCTOBER 2020

©Indian Institute of Technology Delhi (IITD), New Delhi, 2020

**DISPERSION OF VEHICULAR EXHAUST EMISSIONS IN
NEAR-FIELD REGION AROUND FLYOVER IN AN
ENVIRONMENTAL WIND TUNNEL**

by

S. JITENDRA PAL

Department of Civil Engineering

Submitted

In the fulfillment of the requirements of the degree of Doctor of philosophy

to the



INDIAN INSTITUTE OF TECHNOLOGY DELHI

OCTOBER 2020

Dedicated to

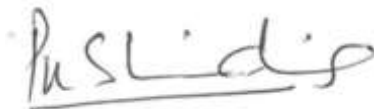
MY LORD

MY PARENTS & FAMILY MEMBERS

CERTIFICATE

This is to certify that the thesis entitled “**Dispersion of vehicular exhaust emissions in near-field region around flyover in an environmental wind tunnel**” being submitted by **Mr. Salavadhi Jitendra Pal** to the Indian Institute of Technology Delhi, New Delhi, for the award of the degree of ‘**Doctor of Philosophy**’ in Department of Civil Engineering is a record of bonafide research work carried out by him under our supervision and guidance. He has fulfilled the requirements for the submission of the thesis, which to the best of our knowledge has reached the requisite standard.

The material contained in the thesis has not been submitted in part or in full to any other University or Institute for the award of any degree or diploma.



Dr. Mukesh Khare

Professor of Environmental Engineering,
Department of Civil Engineering,
IIT Delhi, Hauz Khas,
New Delhi - 110016, India.

Professor Prashant Kumar

Department of Civil and Environmental Engineering,
Professor & Founding Director-GCARE,
The University of Surrey,
Guildford, Surrey, United Kingdom-GU2 7XH.

ACKNOWLEDGEMENTS

I take this opportunity to thank all individuals who have directly or indirectly made the present thesis possible.

Firstly and most importantly, I wish to express my deep sense of gratitude and heartfelt thanks to my thesis advisors, **Professor Mukesh Khare and Professor Prashant Kumar** for their inspiring and ever-positive guidance, critical assessment, unconditional support and help in every possible way. I am grateful to their timely and insightful discussions whenever needed, not just related to research but personal and career guidance. I would especially like to thank my advisors for inculcating and nurturing the essential qualities to become a better researcher and presenter. Under their supervision, I have grown immensely as a researcher and would look forward to their continued mentorship in my career.

I extend my sincere thanks to my Student Research Committee members, Prof. A.K. Gosain (Chairman, SRC) from Department of Civil engineering, Dr. Gazala Habib (Internal Member, SRC) from Department of Civil engineering s and Prof. S. V. Veeravalli (External Member, SRC) from Department of Applied Mechanics, IIT Delhi for their genuine feedback, critical comments and valuable suggestions during the present work. I am obliged to all Heads of the Civil Engineering Department, during my Ph.D. for their constant support.

I am very thankful to the Director, Deans and Head & faculty members of the Department of Chemical Engineering for their constant encouragement, great company and permitting me to pursue my Ph.D. at IIT Delhi.

My sincere gratitude towards Prof. R.M.M. Gowda and Prof. Kafeel Ahmad, who taught me all operations, measurement related techniques and preliminary analysis of wind tunnel related data. My sincere gratitude towards Prof. S. V. Veeravalli, Prof. S. N. Singh, Prof. K.K. Chowdhry & Dr. Murali R. Cholemari from the Department of Applied Mechanics for their valuable

suggestions and insights during my initial stage of Ph.D. and also, for their generosity to allow me to access the Environmental Wind Tunnel (EWT) facility in the Gas dynamics lab.

I am very thankful to Dr. Sanjay Kumar Gupta, Mr. Rajeev Kumar Sharma, Mr. Amit Bundela, Mr. Ishwar Singh & all other Civil Engineering Department staff for their constant encouragement and great company. I want to thank Mr. Kunj Bihari and Mr. Suresh Sharma and Late. Mr. Nanda Lal, the staff of Gas dynamics laboratory, who helped me generously whenever needed for assembling of my models and setup. Heart-full and special thanks to Mr. Sunil Bhogal and Mr. Anwar, who helped me in fabricating my h-MVMS model.

Very special thanks to all my teachers and friends at various academic stages, schooling, college and university for their constant motivation and encouragement. Sincere thanks to Dr. Diwakar, Dr. Sumanth chintala, Dr. Sunil Gulia, Ms. Komal Shukla and Mr. Chandrahas for their discussions related to research and wonderful company. I would also like to thank Dr. Nanjunda Swamy for giving career guidance and motivation.

My sincere gratitude towards all my friends from my heart, who made my stay at IIT Delhi most memorable. I will miss those interesting and long-lasting chats pertaining not just related to research, academics and politics but about everything discussed in the Udaigiri dining table. I express my gratefulness to various Deans and Director, IIT Delhi. The financial assistantship from QIP and the Department of Civil Engineering, IIT Delhi, is highly acknowledged.

Finally, I am forever grateful to my parents, **Mr. Salavadhi Kanakaiah-my father and Late Smt. Sarojini Devi & Late Smt. Venkata Lakshmi**-my lovely & great mother's whom I missed their presence during MyPh.D, for their continued overwhelming support, love, inspiration, encouragement and everything, who has given their today for my better tomorrow. I am highly appreciative of **my wife-Sumalatha, my daughter-Satvika and my son-Raj Kiran**, for their continued support and encouragement. I would sincerely thank my brother S. Jawahar & his family members; Mekala Sanjeev Rao & his family, who have supported me all along the

way. I am indebted and thankful to my uncles, aunties, brothers and sisters of Salavadhi family for their good wishes and blessings.

Finally, I thank the Almighty GOD who has given me this life and helped me throughout my life with joy and health, without GOD, I am nothing.

S. Jitendra Pal

ABSTRACT

Air pollution from motor vehicles is one of the most serious and rapidly growing problems in various urban centers of the world. From the population exposure point of view, the study of air quality in urban street canyons is of paramount importance since the highest pollution levels and considerably larger environmental impacts have often been observed in these situations. To chalk out effective counter-measures for achieving sustainable street air quality, there is a need to analyze the air pollution dispersion phenomenon within the street canyon comprehensively.

Over the past two decades, significant progress has been made in understanding and modelling vehicular pollution dispersion phenomena under these urban environmental conditions by using Environmental Wind Tunnel (EWT) technique. In the EWT, the emission conditions, different meteorological situations, terrain and topographical features could be changed at will and useful data translatable to real-life situations might be obtained. These EWT studies carried out over the last ten years have greatly helped in determining the pollutant concentrations under various urban street canyon conditions as a function of building dimensions, upwind building configuration, wind direction concerning building configuration and roof geometry. These studies have further shown that the street canyon configuration, its aspect ratio, external wind speed and its direction and traffic produced turbulence are some of the important factors influencing pollutant dispersion in urban areas.

In the present study, physical modeling of various street canyon configurations in the EWT facility at the Indian Institute of Technology (IIT) Delhi was carried out to study the heterogeneous traffic-induced effects on pollutant dispersion in street canyon with a flyover. The traffic-induced turbulence, coupled with natural air motions, is an important factor affecting the dispersion of exhaust emissions, especially under low wind conditions. Therefore, a systematic

understanding of the traffic-induced effect on exhaust dispersion mechanisms in the close vicinity of the urban roadways/intersections/street canyons/freeways help in finding ways to mitigate vehicular pollution. Also, an attempt to investigate the effects of building patterns and approaching wind directions on the line source dispersion in the close vicinity of the urban intersection along with flyover was studied. The traffic-induced effects for variable traffic volume, speed and composition have also been investigated. And also, in the present study, forecasting flow fields and concentration patterns in the near-field of a flyover have been investigated. Additionally, the evaluation of vertical spread parameters for various building patterns and approaching wind direction calculated.

A hybrid-model vehicle movement system for an urban intersection having two-way straight, radial peripheral traffic flows and elevated roads has been designed and fabricated in the EWT. The experiments have been carried out in the neutrally stratified atmospheric boundary layer, representing the urban terrain category. The tracer gas concentration has measured, online, at one hundred twenty locations by gas chromatography (FID type detector) at variable approaching wind directions, i.e., 0° , 30° , 60° and 90° and traffic volumes, i.e., no-traffic, lean traffic volume 1200 vehicles/ hr at a speed of 35 km/hr comprising of 10 vehicles/meter length in model and peak traffic volume of 5500 vehicles/hr at a speed of 15 km/hr in the field comprising of 38 vehicles per meter length in wind tunnel tests. Heterogeneous traffic configuration simulated by taking 15 % two-wheelers, 15 % three-wheelers, 5 % buses and 60 % cars at a scale of 1: 100 to generate heterogeneous traffic conditions as seen in the Indian context.

The percentage reduction in normalized concentration (K) values was maximum for an urban road configuration consisting of flyover without buildings/and with downwind side buildings, the percentage decrease is 79 %. For two side building configurations with/and without flyover, the percentage decrease is 50 %. However, the reductions in K values increased with the height of

the building blocks and reached its maximum value of nearly 91 % at the top of the building blocks ($z/H = 0.96$) for all traffic volumes. The study has indicated that under perpendicular and oblique wind directions, pollution distribution in the urban street canyon is affected by the central vortex, whereas, during parallel wind flow, the pollution gets dispersed due to channeling of the flow (Zajic D., 2011) Flow and turbulence in an urban canyon. J. Appl. Meteor. Climatol., 50, 203–223. The effect of traffic produced turbulence reduced significantly with height (z/H). The effect of the vehicle- induced turbulence found to be highest at the pedestrian level, while at sampling locations close to the top edge, the effect of vehicle- induced mixing of pollution observed almost negligible.

The percentage reduction further increased when traffic and wind flow directions were opposite to each other. At the ‘innermost corners’ of the building blocks, facing the intersection, the percentage reductions in ‘K’ were more than at ‘mid’ sections of the building blocks, it may be due to the generation of the corner vortices.

The study has indicated that under perpendicular and oblique wind directions, pollution distribution in the urban street canyon is affected by the central vortex, whereas, during parallel wind flow, the pollution gets accumulated due to channeling of the flow. It is observed that while the increase in traffic increases the pollutant levels in the street canyon, the effect of increased pollution level, to a certain extent, is offset by the increased traffic produced turbulence (TPT) generated by these vehicles.

सार

मोटर वाहनों से वायु प्रदूषण दुनिया के विभिन्न शहरी केंद्रों में सबसे गंभीर और तेजी से बढ़ती समस्याओं में से एक है। जनसंख्या के दृष्टिकोण से, शहरी स्ट्रीट कैनियन में वायु गुणवत्ता का अध्ययन सबसे महत्वपूर्ण है, क्योंकि इन स्थितियों में उच्चतम प्रदूषण का स्तर और काफी बड़ा पर्यावरणीय प्रभाव अक्सर देखा गया है। टिकाऊ सड़क वायु गुणवत्ता को प्राप्त करने के लिए प्रभावी जवाबी उपायों को चाक-चौबंद करने के लिए, सड़क घाटी के भीतर प्रदूषण फैलाव घटना का व्यापक विश्लेषण करने की आवश्यकता है।

पिछले दो दशकों में, पर्यावरणीय पवन सुरंग (EWT) तकनीक का उपयोग करके इन शहरी पर्यावरणीय परिस्थितियों में वाहनों के प्रदूषण फैलाव की घटनाओं को समझने और मॉडलिंग करने में महत्वपूर्ण प्रगति हुई है। EWT में, उत्सर्जन की स्थिति, विभिन्न मौसम संबंधी स्थितियों, इलाके और स्थलाकृतिक विशेषताओं को इच्छाशक्ति में बदला जा सकता है और वास्तविक जीवन की स्थितियों के लिए उपयोगी डेटा का अनुवाद किया जा सकता है। पिछले दस वर्षों में किए गए इन EWT अध्ययनों ने इमारत के आयामों के एक समारोह के रूप में विभिन्न शहरी सड़क घाटी की स्थिति के तहत प्रदूषक सांद्रता को निर्धारित करने में बहुत मदद की है, भवन विन्यास, छत विन्यास और छत ज्यामिति के संबंध में हवा की दिशा। इन अध्ययनों से यह पता चला है कि शहरी क्षेत्रों में प्रदूषक फैलाव को प्रभावित करने वाले कुछ महत्वपूर्ण कारक स्ट्रीट कैनियन कॉन्फिगरेशन, इसका पहलू अनुपात, बाहरी हवा की गति और इसकी दिशा और यातायात से उत्पन्न अशांति कुछ महत्वपूर्ण कारक हैं।

वर्तमान अध्ययन में, भारतीय प्रौद्योगिकी संस्थान (IIT) दिल्ली में EWT सुविधा में विभिन्न सड़क घाटी विन्यासों के भौतिक मॉडलिंग को फ्लाइओवर के साथ सड़क घाटी में प्रदूषक फैलाव पर विषम यातायात-प्रेरित प्रभावों का अध्ययन करने के लिए किया गया है। यातायात-प्रेरित अशांति, प्राकृतिक वायु गतियों के साथ मिलकर एक महत्वपूर्ण कारक है जो विशेष रूप से कम हवा की स्थिति के तहत निकास उत्सर्जन के फैलाव को प्रभावित करता है। इसलिए, शहरी रोडवेज / चौराहों / सड़क घाटियों / फ्रीवेज के निकट

क्षेत्र में निकास फैलाव तंत्र पर यातायात-प्रेरित प्रभाव की एक व्यवस्थित समझ वाहनों के प्रदूषण को कम करने के तरीके खोजने में मदद करती है। इसके अलावा, फ्लाइओवर के साथ-साथ शहरी चौराहे के पास के क्षेत्र में लाइन स्रोत फैलाव पर निर्माण पैटर्न के प्रभाव और हवा के दिशाओं के दृष्टिकोण की जांच करने का प्रयास किया गया है। चर यातायात की मात्रा, गति और संरचना के लिए यातायात-प्रेरित प्रभावों की भी जांच की गई है। और वर्तमान अध्ययन में, एक फ्लाइओवर के निकट क्षेत्र में प्रवाह क्षेत्र और एकाग्रता पैटर्न की भविष्यवाणी की जांच की गई है। इसके अतिरिक्त, विभिन्न भवन पैटर्न और हवा की दिशा के लिए ऊर्ध्वाधर फैल मापदंडों का मूल्यांकन गणना की गई थी।

शहरी चौराहे के लिए दो-तरफ़ा, रेडियल परिधीय यातायात प्रवाह और एलिवेटेड सड़कों के लिए एक हाइब्रिड-मॉडल वाहन आंदोलन प्रणाली को पर्यावरणीय पवन सुरंग (EWT) में डिज़ाइन और निर्मित किया गया है। शहरी इलाके श्रेणी का प्रतिनिधित्व करते हुए, न्यूट्रली स्तरीकृत वायुमंडलीय सीमा परत में प्रयोग किए गए हैं। ट्रेसर गैस की सांद्रता को गैस क्रोमैटोग्राफी (FID प्रकार डिटेक्टर) द्वारा एक सौ बीस स्थानों पर, हवा के दिशा-निर्देश पर, अर्थात्, 0°, 30°, 60° और 90°, और नो-ट्रैफ़िक के माध्यम से मापा जाता है।, 35 किमी / घंटा की गति से दुबला ट्रैफ़िक वॉल्यूम 1200 वाहन / घंटा, जिसमें 10 वाहन / मीटर की लंबाई मॉडल और शिखर ट्रैफ़िक वॉल्यूम 5500 वाहन / घंटा की गति से 15 किमी / घंटा की गति से 38 वाहन शामिल हैं। पवन सुरंग परीक्षणों में मीटर की लंबाई। विषम ट्रैफ़िक कॉन्फ़िगरेशन को 15% दोपहिया, 15% तिपहिया वाहनों, 5% बसों और 60% कारों को 1: 100 के पैमाने पर ले लिया गया था, ताकि भारतीय संदर्भ में देखा जा सके।

सामान्य शहरीकरण (के) मूल्यों में प्रतिशत में कमी एक शहरी सड़क विन्यास के लिए अधिकतम थी जिसमें इमारतों के बिना फ्लाइओवर शामिल था / और नीचे की ओर इमारतों के साथ, प्रतिशत की कमी 79 प्रतिशत है। / और बिना फ्लाइओवर के दो साइड बिल्डिंग कॉन्फ़िगरेशन के लिए, प्रतिशत में कमी 50 प्रतिशत है। हालाँकि, K मूल्यों में कटौती बिल्डिंग ब्लॉक्स की ऊंचाई के साथ बढ़ी और सभी ट्रैफ़िक

वॉल्यूम के लिए बिल्डिंग ब्लॉक्स ($z / Z = 0.96$) के शीर्ष पर इसकी अधिकतम कीमत लगभग 91% तक पहुंच गई। अध्ययन ने संकेत दिया है कि लंबवत और तिरछी हवा के निर्देशों के तहत, शहरी सड़क घाटी में प्रदूषण वितरण केंद्रीय भंवर से प्रभावित होता है, जबकि समानांतर हवा के प्रवाह के दौरान, प्रवाह के चैनलिंग के कारण प्रदूषण फैल जाता है। ट्रेफिक निर्मित अशांति का प्रभाव ऊंचाई (z / H) के साथ काफी कम हो गया। वाहन-प्रेरित मिश्रण का प्रभाव पैदल यात्री के स्तर पर अधिकतम पाया गया, जबकि शीर्ष किनारे के निकट के स्थानों पर, वाहन-प्रेरित मिश्रण के प्रदूषण का प्रभाव लगभग नगण्य पाया गया।

ट्रेफिक और हवा के प्रवाह की दिशा एक-दूसरे के विपरीत होने पर प्रतिशत में कमी आई। भवन ब्लॉकों के At अंतरतम कोनों 'पर, चौराहे का सामना करते हुए,' K 'में प्रतिशत में कमी इमारत ब्लॉकों के मध्य' वर्गों से अधिक थी, यह कोने के भंवर की पीढ़ी के कारण हो सकता है। अध्ययन ने संकेत दिया है कि लंबवत और तिरछी हवा के निर्देशों के तहत, शहरी सड़क घाटी में प्रदूषण वितरण केंद्रीय भंवर से प्रभावित होता है, जबकि समानांतर हवा के प्रवाह के दौरान, प्रवाह के चैनलिंग के कारण प्रदूषण फैल जाता है। यह पाया गया कि यातायात में वृद्धि से सड़क घाटी में प्रदूषक स्तर बढ़ जाता है, प्रदूषण स्तर में वृद्धि का प्रभाव कुछ हद तक इन वाहनों द्वारा उत्पन्न यातायात में वृद्धि हुई अशांति (टीपीटी) से होता है।

TABLE OF CONTENTS

CERTIFICATE	i
ACKNOWLEDGEMENTS	iii
ABSTRACT	vii
TABLE OF CONTENTS	xi
LIST OF FIGURES	xv
LIST OF TABLES	xxi
LIST OF ABBREVIATIONS	xxiii
CHAPTER 1: INTRODUCTION	1
1.1 General	1
1.2 Statement of the problem	2
1.3 Motivation for the present study	3
1.4 Wind tunnel simulations.....	4
1.5 Scope and objectives	5
CHAPTER 2: LITERATURE REVIEW	6
2.1 General	6
2.2 Physical modelling in EWT	6
2.2.1 Advantages of wind tunnel modelling	6
2.3 Atmospheric Boundary Layer (ABL)	7
2.3.1 Characteristics of ABL.....	9
2.3.2 Turbulence Intensity and Reynolds stresses.....	12
2.3.3 Integral length scale	13
2.3.4 Power spectral density function	14
2.3.5 Simulation techniques of ABL in EWT	15
2.4 Similarity criteria in EWT.....	17
2.4.1 Reynolds number.....	19
2.4.2 The similarity in vehicular exhaust emissions	21
2.4.3 Relaxations in vehicular exhaust emission similarities.....	22

2.5	Dispersion studies in street canyon	23
2.5.1	Flow field around structures.....	23
2.5.2	Isolated buildings:	24
2.5.3	Group of buildings	27
2.5.4	Wind tunnel modelling of street canyons.....	29
2.6	Dispersion parameters	34
2.7	Line source simulation	38
2.8	Simulation of traffic and vehicle movement systems	40
2.9	Studies on vehicular motion and turbulence	43
2.9.1	Traffic induced turbulence modelling (Depaul et al., 1986).....	46
2.9.2	Plate similarity criteria for modelling of moving traffic	47
CHAPTER 3: EXPERIMENTAL SETUP		50
3.1	Design considerations of EWT	50
3.2	Details of EWT facility	51
3.3	Hot-wire probe calibration	54
3.4	Calibration of EWT.....	55
3.5	ABL Simulation	56
3.5.1	The mean vertical velocity	57
3.5.2	Turbulence profile.....	62
3.5.3	Simulation of the Urban-intersection	63
3.6	Simulation of the Hybrid-Model Vehicle Movement System (h-MVMS)	63
3.6.1	Traffic simulation at ground level.....	66
3.6.2	Traffic simulation on the flyover	66
3.6.3	Special features of the h-MVMS.....	69
3.7	Simulation of line source.....	70
3.8	Experimental methodology	72
3.9	Gas-Chromatograph Calibration	73
CHAPTER 4: EXPERIMENTAL PROCEDURE.....		75
4.1	General physical modelling studies.....	75
4.2	Meteorological parameters.....	75
4.3	Traffic parameters	76

4.4	Location of sampling points	76
4.5	Tracer gas sampling technique	77
4.6	Test parameters used in the study	79
CHAPTER 5: RESULTS AND DISCUSSION		80
5.1	General	80
5.2	Effects of surrounding building blocks on the line source dispersion at $\theta = 90^\circ$ approaching perpendicular wind direction	80
5.2.1	Line source dispersion for plain road configuration without flyover, $\theta = 90^\circ$	80
5.2.3	Line source dispersion for two side buildings configuration without flyover, $\theta = 90^\circ$	85
5.2.5	Line source dispersion for a flyover without surrounding buildings configuration, $\theta = 90^\circ$	89
5.2.7	Line source dispersion for a flyover with downwind side buildings configuration, $\theta = 90^\circ$	91
5.2.9	Line source dispersion for a flyover with two side buildings configuration. $\theta = 90^\circ$	94
5.2.11	Effect of surrounding building blocks at each location, $\theta = 90^\circ$	98
5.2.12	Overall summary of the effect of surrounding building blocks in the near field region of a flyover at $\theta = 90^\circ$ approaching perpendicular wind direction	101
5.3	Effects of simulated urban road configurations with surrounding buildings and flyover for various approaching wind directions near line source dispersion	102
5.3.1	Effects of surrounding building blocks at oblique-angle approaching wind direction, $\theta = 60^\circ$	102
5.3.3	Effects of building blocks at oblique-angle approaching wind direction $\theta = 30^\circ$	107
5.3.5	Effects of building blocks at Parallel approaching wind direction, $\theta = 0^\circ$..	112
5.3.7	Effect of approaching wind direction on the simulated urban intersection at various locations	118
5.3.8	Overall summary of the effect of approaching wind direction on the simulated urban intersection	121
5.4	Effect of various traffic densities at a particular wind directions	123
5.4.1	Effect of traffic at parallel approaching wind directions, $\theta = 0^\circ$	125
5.4.3	Effect of traffic at oblique approaching wind directions, $\theta = 30^\circ$	129
5.4.5	Effect of traffic at oblique approaching wind directions, $\theta = 60^\circ$	134
5.4.7	Effect of traffic at perpendicular approaching wind directions, $\theta = 90^\circ$	139

5.4.9 Overall summary of the effect of approaching wind direction on the simulated urban intersection	144
5.5 Comparison of σ_z variation for various building patterns and approaching wind directions	145
5.5.1 Effect of surrounding building blocks.....	145
5.5.2 Effects of simulated urban road configurations for various approaching wind directions.....	146
CHAPTER 6: CONCLUSIONS	148
6.1 General	148
6.2 Effects of Surrounding buildings	148
6.3 Effects of Approaching wind directions.....	149
6.4 Effects of traffic volume along with approaching wind directions.....	151
6.5 Estimation of σ_z values for different terrain configurations and approaching wind directions	152
6.6 Contributions of the present study	153
6.7 Recommendations for future work.....	155
REFERENCES.....	157
BIODATA OF THE AUTHOR.....	178

LIST OF FIGURES

Figure 2.1 Schematic diagram showing processes, flow and scale lengths within an urban boundary layer (Fisher et al., 2005).....	8
Figure 2.2: Longitudinal velocity profiles over uniform terrain in neutral flow (Cochran, 2002).....	11
Figure 2.3 Profiles of Turbulent Intensity in Neutral Flow over Uniform Terrain (Cochran, 2002).....	14
Figure 2.4 Scheme of the comparison (Baechlin et al., 1991).....	19
Figure 2.5 Flow near a sharp-edged three-dimensional building in a deep boundary layer (Hosker, 1984).....	25
Figure 2.6 Main features of flow around cuboids at 0° and 45° to the approach flow in a deep boundary layer (Ahmad, 2004).....	26
Figure 2.7 Scheme of pollutant dispersion paths in the simplified street canyon (Pospisil et al., 2017).....	29
Figure 2.8 Schematic of the flow regimes (Oke, 1988) with height H and separation S_1	31
Figure 2.9 Flow structures around buildings and inside a long street canyon with (a) perpendicular, (b) oblique and (c) parallel wind flow. (Yazid, et al., 2014).....	32
Figure 3.1 Layout of EWT at IIT Delhi.....	51
Figure 3.2 A typical calibration curve of hot-wire probe calibration.....	54
Figure 3.3 A typical curve showing wind tunnel flow speeds at different frequencies of the motor controller.....	55
Figure 3.4 A typical curve showing the longitudinal velocity profiles at various elevations.....	56
Figure 3.5 Elevation and plan view of EWT along with simulated ABL along with roughness generating devices of EWT.....	57
Figure 3.6 Passive devices arrangement in the EWT.....	58
Figure 3.7 (Plate 3.1) Picture showing ABL generating devices, simulated urban intersection and traversing mechanism.....	58

Figure 3.8 Normalized longitudinal mean velocity profile at 11 m.....	59
Figure 3.9 Comparison of longitudinal turbulence intensity (a) normalized, (b) full-scale. . .	62
Figure 3.10 Simulated urban intersection in the EWT.	64
Figure 3.11 (Plate 3.2) Picture showing simulated urban intersection with flyover side and top view.....	65
Figure 3.13 Sectional elevation of the h-MVMS system.....	67
Figure 3.14 Plan-view of h-MVMS at ground level.....	68
Figure 3.15 Pictorial view of vehicle movement on flyover.....	68
Figure 3.16 Side view of line source.	71
Figure 3.17 Tracer dispersion experimental setup.....	73
Figure 3.18 A typical GC calibration curve.....	74
Figure 4.1 Location of sampling point at urban intersection in (a) Horizontal and (b) Vertical plane.....	78
Figure 5.1 Detailed description of sampling point locations in the horizontal plane at, $\theta = 90^\circ$	81
Figure 5.2 Variation of normalized vertical concentration profiles on the upwind side of the plain street, $\theta = 90^\circ$	83
Figure 5.3 Variation of normalized vertical concentration profiles on the downwind side of the plain street, $\theta = 90^\circ$	83
Figure 5.4 Variation of normalized vertical concentration profiles in the perpendicular downwind plain street, $\theta = 90^\circ$	84
Figure 5.5 Variation of normalized vertical concentration profiles in the downwind central line of the plain street, $\theta = 90^\circ$	85
Figure 5.6 Variation of normalized vertical concentration profiles on the leeward side wall of the street canyon without flyover, $\theta = 90^\circ$	88

Figure 5.7 Variation of normalized vertical concentration profiles on the windward side wall of the street canyon without flyover, $\theta = 90^\circ$	88
Figure 5.8 Variation of normalized vertical concentration profiles on downwind street wall of the street canyon without flyover, $\theta = 90^\circ$	88
Figure 5.9 Variation of normalized vertical concentration profiles on the downwind central line of the street canyon without flyover, $\theta = 90^\circ$	89
Figure 5.10 Variation of normalized vertical concentration profiles on the upwind side of the flyover without surrounding buildings, $\theta = 90^\circ$	91
Figure 5.11 Variation of normalized vertical concentration profiles on the downwind side of the flyover without surrounding buildings, $\theta = 90^\circ$	91
Figure 5.12 Variation of normalized vertical concentration profiles on downwind street of the flyover without surrounding buildings, $\theta = 90^\circ$	92
Figure 5.13 Variation of normalized vertical concentration profiles on the downwind central line of the flyover without surrounding buildings, $\theta = 90^\circ$	92
Figure 5.14 Variation of normalized vertical concentration profiles on the upwind side of the flyover with downwind side buildings, $\theta = 90^\circ$	94
Figure 5.15 Variation of normalized vertical concentration profiles on the downwind side of the flyover with downwind side buildings, $\theta = 90^\circ$	94
Figure 5.16 Variation of normalized vertical concentration profiles on downwind street of the flyover with downwind side buildings, $\theta = 90^\circ$	94
Figure 5.17 Variation of normalized vertical concentration profiles on the downwind central line of the flyover with downwind side buildings, $\theta = 90^\circ$	95
Figure 5.18 Variation of normalized vertical concentration profiles on the leeward side of the flyover with two side buildings, $\theta = 90^\circ$	96
Figure 5.19 Variation of normalized vertical concentration profiles on the windward side of the flyover with two side buildings, $\theta = 90^\circ$	96
Figure 5.20 Variation of normalized vertical concentration profiles in downwind street inner walls of the flyover with two side buildings, $\theta = 90^\circ$	97
Figure 5.21 Variation of normalized vertical concentration profiles in the downwind central line of the flyover with two side buildings, $\theta = 90^\circ$	97
Figure 5.22 Variation of normalized vertical concentration profiles at various sections on	

leeward side, $\theta = 90^\circ$	98
Figure 5.23 Variation of normalized vertical concentration profiles at various sections on windward side, $\theta = 90^\circ$	99
Figure 5.24 Variation of normalized vertical concentration profiles at various sections in downwind street, $\theta = 90^\circ$	100
Figure 5.25 Variation of normalized vertical concentration profiles at various sections in downwind central line, $\theta = 90^\circ$	101
Figure 5.26 Detailed description of sampling point locations of the simulated urban intersection at oblique approaching wind direction, $\theta = 60^\circ$	103
Figure 5.27 Variation of normalised vertical concentration profiles on the leeward side of the flyover with two side buildings, $\theta = 60^\circ$	106
Figure 5.28 Variation of normalised vertical concentration profiles on the windward side of the flyover with two side buildings, $\theta = 60^\circ$	106
Figure 5.29 Variation of normalised vertical concentration profiles on downwind street of the flyover with two side buildings, $\theta = 60^\circ$	107
Figure 5.30 Variation of normalised vertical concentration profiles on the downwind central line of the flyover with two side buildings, $\theta = 60^\circ$	107
Figure 5.31 Detailed description of sampling point locations of the simulated urban intersection at oblique approaching wind direction, $\theta = 30^\circ$	108
Figure 5.32 Variation of normalised vertical concentration profiles on the leeward side of the flyover with two side buildings, $\theta = 30^\circ$	111
Figure 5.33 Variation of normalised vertical concentration profiles on the windward side of the flyover with two side buildings, $\theta = 30^\circ$	111
Figure 5.34 Variation of normalised vertical concentration profiles on downwind street of the flyover with two side buildings, $\theta = 30^\circ$	112
Figure 5.35 Variation of normalised vertical concentration profiles on the downwind central line of the flyover with two side buildings, $\theta = 30^\circ$	112
Figure 5.36 Detailed description of sampling point locations of the simulated urban intersection at parallel approaching wind direction, $\theta = 0^\circ$	113
Figure 5.37 Variation of normalised vertical concentration profiles on the leeward side of the flyover with two side buildings, $\theta = 0^\circ$	116

Figure 5.38 Variation of normalised vertical concentration profiles on the windward side of the flyover with two side buildings, $\theta = 0^\circ$	116
Figure 5.39 Variation of normalised vertical concentration profiles on downwind street of the flyover with two side buildings, $\theta = 0^\circ$	117
Figure 5.40 Variation of normalised vertical concentration profiles on the downwind central line of the flyover with two side buildings, $\theta = 0^\circ$	117
Figure 5.41 Variation of normalised vertical concentration profiles with various wind directions at various sections on the leeward side of the flyover with two side buildings	118
Figure 5.42 Variation of normalised vertical concentration profiles with various wind directions at various sections on the windward side of the flyover with two side buildings.	119
Figure 5.43 Variation of normalised vertical concentration profiles with various wind directions at various sections on the downwind side of the flyover with two side buildings	120
Figure 5.44 Variation of normalised vertical concentration profiles with various wind directions at various sections on downwind central lineside of the flyover with two side buildings.....	120
Figure 5.45 Detailed description of sampling point locations of the simulated urban intersection at parallel approaching wind direction, $\theta = 0^\circ$	125
Figure 5.46 Variation of normalised vertical concentration profiles on leeward side wall showing traffic induced effect, $\theta = 0^\circ$	127
Figure 5.47 Variation of normalised vertical concentration profiles on windward side wall showing traffic induced effect, $\theta = 0^\circ$	128
Figure 5.48 Variation of normalised vertical concentration profiles on downwind street inner side wall showing traffic-induced effect, $\theta = 0^\circ$	129
Figure 5.49 Detailed description of sampling point locations of the simulated urban intersection at oblique approaching wind direction, $\theta = 30^\circ$	130
Figure 5.50 Variation of normalised vertical concentration profiles on leeward side wall showing traffic-induced effect, $\theta = 30^\circ$	132
Figure 5.51 Variation of normalised vertical concentration profiles on windward side wall showing traffic-induced effect, $\theta = 30^\circ$	133
Figure 5.52 Variation of normalised vertical concentration profiles on downwind street inner side wall showing traffic-induced effect, $\theta = 30^\circ$	134

Figure 5.53 Detailed description of sampling point locations of the simulated urban intersection at oblique approaching wind direction, $\theta = 60^\circ$	135
Figure 5.54 Variation of normalised vertical concentration profiles on leeward side wall showing traffic induced effect, $\theta = 60^\circ$	137
Figure 5.55 Variation of normalised vertical concentration profiles on windward side wall showing traffic induced effect, $\theta = 60^\circ$	138
Figure 5.56 Variation of normalised vertical concentration profiles on downwind street inner side wall showing traffic induced effect, $\theta = 60^\circ$	139
Figure 5.57 Detailed description of sampling point locations of the simulated urban intersection at perpendicular approaching wind direction, $\theta = 90^\circ$	140
Figure 5.58 Variation of normalised vertical concentration profiles on leeward side wall showing traffic induced effect, $\theta = 90^\circ$	141
Figure 5.59 Variation of normalised vertical concentration profiles on windward side wall showing traffic induced effect, $\theta = 90^\circ$	142
Figure 5.60 Variation of normalised vertical concentration profiles on downwind street inner side wall showing traffic-induced effect, $\theta = 90^\circ$	143
Figure 5.61 Variation of σ_z in a downwind central line for various surrounding buildings arrangement for the simulated urban intersection.....	146
Figure 5.62 Variation of σ_z in downwind central line at various approaching wind directions for the simulated urban intersection.....	147

LIST OF TABLES

Table 2.1	Value s of δ and α for representative topography (Sivaramakrishnan, 1980).....	13
Table 2.2	Similarity Criteria (Snyder, 1981).....	20
Table 2.3	Empirical Constants (Chock, 1978).....	35
Table 3.1	Estimated ABL roughness factors.	60
Table 3.2	Evaluation of roughness parameters.	61
Table 3.3	Typical dimensions of the model vehicle.	69
Table 3.4	Typical simulated model vehicle volume.	70
Table 3.5	Typical model vehicle Speeds.	70
Table 3.6	Tracer gases used in the earlier studies as per the literature.	72
Table 4.1	Major test parameters for wind tunnel experimentations.	79

LIST OF ABBREVIATIONS

EWT	Environmental wind tunnel
ABL	Atmospheric boundary layer
MVMS	Model Vehicle Movement System
<i>f</i> - MVMS	The flexible model vehicle movement system
h-MVMS	The hybrid-model vehicle movement system
MMR	Moving model rig
ARMA	Autoregressive moving average
DC	Direct current
HP	Horsepower
H/W	Height to width ratio
L/H	Length to height ratio
m/s	Meter/second
km/hr	Kilometer/hour
ESDU	Engineering sciences data unit (U.K)
EPA	Environmental Protection Agency
RCC	Reinforced cement concrete
M.S.	Mild steel
ASCE	American society of civil engineers
Re	Reynolds number
GC	Gas chromatograph
FID	Flame ionization detector